Brazilian Journal of Medical and Biological Research (2002) 35: 895-903
ISSN 0100-879X

Measurement of the ultrasonic properties of human coronary arteries *in vitro* with a 50-MHz acoustic microscope

J.C. Machado[1], F.S. Foster[2] and A.I. Gotlieb[3]

[1]Programa de Engenharia Biomédica, COPPE, Universidade Federal do Rio de Janeiro, Rio de Janeiro, RJ, Brasil
[2]Sunnybrook and Women's College Health Sciences Centre, Department of Medical Biophysics, University of Toronto, Toronto, Ontario, Canada
[3]Vascular Research Laboratory, Department of Laboratory Medicine and Pathobiology, Banting and Best Diabetes Centre, The Toronto Hospital Research Institute, University of Toronto, Toronto, Ontario, Canada

Abstract

Ultrasonic attenuation coefficient, wave propagation speed and integrated backscatter coefficient (IBC) of human coronary arteries were measured *in vitro* over the -6 dB frequency bandwidth (36 to 67 MHz) of a focused ultrasound transducer (50 MHz, focal distance 5.7 mm, f/number 1.7). Corrections were made for diffraction effects. Normal and diseased coronary artery sub-samples (N = 38) were obtained from 10 individuals at autopsy. The measured mean ± SD of the wave speed (average over the entire vessel wall thickness) was 1581.04 ± 53.88 m/s. At 50 MHz, the average attenuation coefficient was 4.99 ± 1.33 dB/mm with a frequency dependence term of 1.55 ± 0.18 determined over the 36- to 67-MHz frequency range. The IBC values were: 17.42 ± 13.02 $(sr.m)^{-1}$ for thickened intima, 11.35 ± 6.54 $(sr.m)^{-1}$ for fibrotic intima, 39.93 ± 50.95 $(sr.m)^{-1}$ for plaque, 4.26 ± 2.34 $(sr.m)^{-1}$ for foam cells, 5.12 ± 5.85 $(sr.m)^{-1}$ for media and 21.26 ± 31.77 $(sr.m)^{-1}$ for adventitia layers. The IBC results indicate the possibility for ultrasound characterization of human coronary artery wall tissue layer, including the situations of diseased arteries with the presence of thickened intima, fibrotic intima and plaque. The mean IBC normalized with respect to the mean IBC of the media layer seems promising for use as a parameter to differentiate a plaque or a thickened intima from a fibrotic intima.

Correspondence
J.C. Machado
Programa de Engenharia Biomédica
COPPE, UFRJ
Caixa Postal 68510
21945-970 Rio de Janeiro, RJ
Brasil
Fax: +55-21-2562-8591
E-mail: jcm@peb.ufrj.br

Research supported by PRONEX/FINEP, CAPES, Universidade Federal do Rio de Janeiro, and the Medical Research Council of Canada.
F.S. Foster is a Terry Fox Scientist of the National Cancer Institute of Canada.

Received August 29, 2001
Accepted May 29, 2002

Key words
- Acoustic microscopy
- Coronary artery wall
- Ultrasound tissue characterization
- Integrated backscatter coefficient

Introduction

Atherosclerosis, a disease of the arterial wall, is the most common vascular disease in Western society. It is characterized by the formation of plaques that range from early stage lesions or fatty streaks to complex late stage lesions that may contain fibrous tissue, extracellular lipids, cholesterol, necrotic cellular debris, calcification, and regions of incorporated thrombus (1). Atherosclerotic plaques become clinically manifest when they have reached the stage of the fibrous-fatty or complicated plaque and significantly encroach on the vessel lumen. In advanced stages, acute events result in sudden vessel

occlusion, most commonly due to the formation of thrombus after plaque fracture or rupture (2).

The procedure to treat diseased arteries with atherosclerotic plaque requires not only visualization of the lesion, but also characterization of the plaque contents. Conventional approaches such as X-ray contrast angiography permit excellent visualization of the lumens of critical arteries such as the coronaries but provide limited information on the structure and properties of any plaque that may be present (3). On the other hand, considerable evidence now exists to conclude that intravascular ultrasound imaging is a more sensitive indicator of calcium content, residual plaque burden, tissue trauma, and final lumen dimensions than angiography (4,5).

Ultrasonic characterization of vascular tissue has evolved from the use of frequencies between 4 and 15 MHz, (6-8) to the 20- to 27-MHz range (9,10), and more recently between 25 and 65 MHz (11-13). The benefits of using higher frequencies are the improvement of image quality as well as of the characterization of the layered structure of the vessel wall and consequently of the atherosclerotic plaque. Although most of the current intravascular ultrasound machines operate close to 30 MHz, recent commercial prototype systems offer the option to operate at both 30 and 40 MHz (14).

Despite the development of intravascular ultrasound machines operating at frequencies higher than 30 MHz, our understanding of the scattering and attenuation processes in normal and diseased coronary arteries is very limited. Also, the relative levels of backscatter from critical structures such as early and late thrombus, soft or fibrous plaque, blood, and intima, media and adventitia layers are not well understood, particularly in the high frequency range. Previous studies refer to *in vitro* characterization of human carotid (11) and femoral arteries (11,13,15) and to the quantification of the lipid-rich intima layer of atherosclerotic rabbit aortas (12).

The present study reports absolute measurements of ultrasonic backscattering properties of human coronary artery walls, by means of the integrated backscatter coefficient (IBC) as a function of depth in the vessel wall. The IBC reflects the acoustic characteristic of the tissue related to its capacity of sending backwards an acoustic power in response to an incident wave.

A recent study by Machado and Foster (16) developed the basic formulation and the setup used for experimental measurement of the IBC profile of human coronary arteries *in vitro*. The method was tested with three samples of vessel wall. The present study applies the method to a larger number of vessel samples, including different types of plaque on the arterial wall.

Data were obtained at 50 MHz and with a population of 38 vessel wall samples of *ex vivo* coronary arteries containing histological findings of thickened intima, fibrotic intima, plaques and foam cells. Appropriate diffraction correction was implemented to compensate for the diffraction effects imposed by the spherically focused ultrasonic transducer operating with a center frequency of 50 MHz and an f/number of 1.7. Data for average wave speed and average attenuation coefficient, at 50 MHz, across the vessel wall are also presented.

Material and Methods

Sample preparation

Ten samples, either right or left anterior descending coronary artery, were obtained immediately following autopsy of males and females ranging in age from 38 to 88 years. The tissue was frozen at -32ºC until use. Previous investigators have shown that freezing and thawing has only minimal effects on the ultrasound parameters of some human tissues (17,18). Subsequent to the ultrasonic measurements, these samples were fixed in

formalin and paraffin embedded, and sections were stained with Movat stain for histological analysis. Photographs of the sections, printed with a magnification close to the ultrasound biomicroscope (UBM) images, were prepared for comparison with the ultrasound images and for determination of the layers present on the wall.

Prior to the ultrasound measurements, the samples were brought to room temperature and a sub-sample measuring approximately 2 x 3 mm was cut and placed in the sample holder. Table 1 presents a list of all the samples together with the sub-samples they provided. The histological result for each sub-sample is also given in the table.

Table 1. Coronary artery samples used in the present study with patient age and related sub-samples, defined by a number, classified according to their histological results.

Sample	Age (years)	Sub-sample number and histological result				N_S
		Thickened intima	Fibrotic intima	Plaque presence	Foam cell presence	
I	77	1, 2	25, 26, 27, 28	25, 26, 27, 28		6
II	39	3, 4, 5, 6	29			5
III	38	7, 8, 9, 10, 11, 12	30, 31			8
IV	64	13, 14, 15, 16, 17		13, 14, 15	13, 14, 15	5
V	73	18, 19	34, 35	19		4
VI	67	20		20		1
VII	73	21, 22	36	37		4
VIII	73	23, 24				2
IX	79		32, 33	33		2
X	88			38		1
Amount		25	12	12	3	38

N_S = the number of sub-samples from the same sample. Right coronary arteries are: I, II, III, IV, IX, and left anterior descending coronary arteries are: V, VI, VII, VIII, X.

Measurement system

An overview block diagram depicting the experimental setup is presented in Figure 1A, whereas the details of the sample holder are shown in Figure 1B. The measurement system consisted of a UBM working with a focused polyvinylidene fluoride transducer (receiving solid angle of 0.27 sr, aperture of 3.1 mm, focal depth of 5.7 mm, center frequency f_c = 50 MHz and -6 dB frequency bandwidth of 36 to 67 MHz). Figure 2 shows the frequency spectrum of the pulse transmitted by the transducer which was obtained from the echo from a quartz plate positioned at the focus and perpendicular to the beam axis. A review of ultrasound biomicroscopy is given by Foster et al. (19).

A temperature-controlled micropositioned tissue cell was used for data collection. The artery samples, placed over a flat quartz plate with the intima layer upwards, were covered with a 15-µm thick resinite membrane (AEP Industries Inc., West Hill, ON, Canada) and immersed in saline at 37ºC. The adjustable height platform allowed adjustment of the necessary contact pressure between the sample and the membrane to anchor the sample and maintain a flat surface. Prior to data acquisition, the UBM

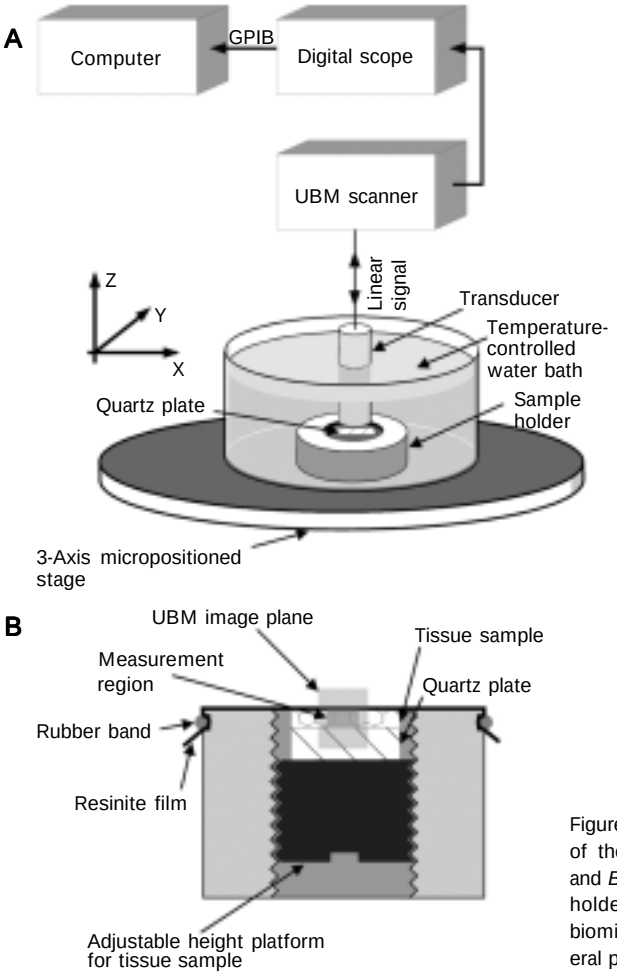

Figure 1. *A*, Block diagram of the experimental setup and *B*, detail of the sample holder. UBM, ultrasound biomicroscope; GPIB, general purpose interface bus.

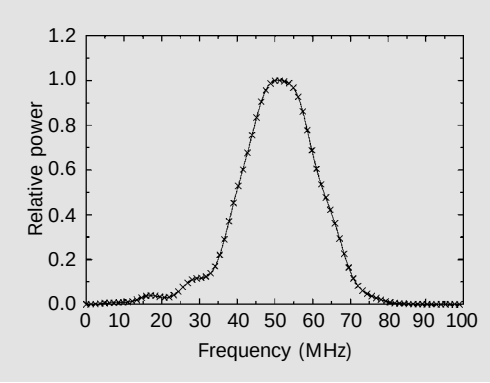

Figure 2. Frequency spectrum of the ultrasonic pulse reflected from the quartz plate positioned at the transducer focus and perpendicular to the beam axis. Data were normalized to the maximum.

scanner provided overview images of the membrane to insure the flatness of its surface and of the tissue microstructure to provide accurate targeting of homogeneous tissue regions for quantitative analysis. The front end of the UBM scanner was fixed to a three-axis micropositioning system to permit accurate data acquisition.

The rf signals resulting from reflections on the membrane and quartz surface plus backscattering from the tissue were recorded using a digital oscilloscope and collected from 64 positions over an 8 x 8 matrix with a 50-µm separation. In order to collect the rf signal over the sample thickness, the signal window on the oscilloscope was 1 µs (≅ 787.5 µm) for narrow samples, and 2 µs (≅ 1575 µm) for wider ones. These settings provided sampling frequencies of 1000 and 500 MHz, respectively. The sampled rf signals were transferred by a general purpose interface bus to the microcomputer for further processing and calculations.

The rf-backscattered signals were compensated for attenuation using an inverse attenuation filter as described by D'Astous and Foster (17). The resulting signal $V_s(t)$ was squared and the product passed through a 4th order low-pass Butterworth filter (cut-off at 50 MHz) to eliminate the high frequency components. The filter output provided 64 signals of the $U_s(x_i,y_j,t)$ form with coordinates x_i and y_j ($1 \le i,j \le 8$) on a plane perpendicular to the transmitted beam z-axis. The mean acoustic power backscattered from a region inside the sample and at a depth $\bar{r}$ (= $ct/2$ and c = wave speed) is proportional to the mean rf-backscattered power signal, and is determined as:

$$\left\langle |V_s(\bar{r})|^2 \right\rangle = \frac{1}{64} \sum_{i=1}^{8} \sum_{j=1}^{8} U_s(x_i, y_j, \bar{r}) \quad \text{Equation 1}$$

The IBC as a function of depth, $IBC(\bar{r})$, is obtained from Equation 1 after normalizing $\left\langle |V_s(\bar{r})|^2 \right\rangle$ with the transducer receiver solid angle, the diffraction correction function, the acoustic wave speed and the incident acoustic energy. After normalization, the result must also be corrected for the effects of a focused beam reflected on a flat plane. Details about the calculation of $IBC(\bar{r})$ from $\left\langle |V_s(\bar{r})|^2 \right\rangle$ are presented in Ref. 16.

Wave speed, sample thickness and attenuation coefficient were calculated using the approaches previously described by Lockwood et al. (11) and Ye et al. (20). The mean values of the wave speed along the sample wall, of the wall thickness and of the attenuation coefficient were obtained by averaging the corresponding values obtained from the 64 measurements.

For most soft tissues and body liquids, the frequency dependence of attenuation $\alpha(f)$ can be expressed as:

$$\alpha(f) = \alpha_0 f^{\gamma} = \alpha_0 f_c^{\gamma} \left(\frac{f}{f_c} \right)^{\gamma} \quad \text{Equation 2}$$

where f is the ultrasonic frequency, α_0 is the attenuation coefficient at 1 MHz and γ is the frequency dependence, usually between 1 and 2. The attenuation coefficient at transducer center frequency is $\alpha_c = \alpha_0 f_c^{y}$.

Results

The IBC profile was obtained for the 38 coronary artery sub-samples presented in Table 1. Three examples of the plots for the IBC are presented: one with a mildly thickened intima, in Figure 3a, one with both

thickened intima and a plaque, Figure 4a, and the third one, in Figure 5a, with a highly significantly thickened intima. Figures 3b-5b and 3c-5c correspond to the UBM and histological images, respectively. In both figures, the segment of the IBC plot corresponding to either a plaque or a tissue wall layer contains a darker line. Localization and definition of the length of each segment were determined considering the relative dimensions of each layer in both UBM and histological images. In most situations, the media layer was the easiest to identify due to the marked peaks caused by the strong backscattering from both the internal and external elastic lamina at the IBC plots.

The results for the IBC layer segment of each sub-sample were determined and are reported as mean ± SD. In Figure 6A they are presented for the intima, media and adventitia layers of the 24 sub-samples containing only thickened intima. Similar results are also presented in Figure 6B for the 12 sub-samples containing a fibrotic intima. Figure 6C contains similar plots for the plaque, media and adventitia layers of the 12 sub-samples with plaque, and Figure 6D illustrates the results for plaque containing foam cells, media and adventitia layers of sub-samples 13, 14 and 15.

The ratio between the mean IBC for one of the innermost layers (thickened intima, fibrotic intima, plaque or foam cell) and the mean IBC of the media layer belonging to the same sub-sample was calculated. The result, presented in Figure 7, is expressed in terms of the mean and standard deviation of the IBC ratio distribution for each group: thickened intima, fibrotic intima, plaque and foam cells. These results allow us to compare the scattering strength of one of the innermost layer to the media layer of the same sub-sample, independently of the individual artery samples. On average, the plaque layer scatters 8 times more than the media layer, the thickened intima 5 times more, the fibrotic intima 2.5 times more and the foam cells 1.9 times more.

Wave speed (c), attenuation coefficient at 50 MHz (α_c) and the frequency dependence term (γ) of the attenuation coefficient did not present any correlation with the presence or absence of thickened intima, fibrotic intima, plaque or foam cells on the artery wall. Mean ± SD for c, α_c, and γ were measured over the sub-sample population (N = 38) and the results were 1581.04 ± 53.88 m/s, 4.99 ± 1.33 dB/mm and 1.55 ± 0.18, respectively.

Discussion

Ultrasound was used at 50 MHz to characterize the tissue wall of *ex vivo* human coronary arteries. The results, presented in terms of ultrasound wave speed, attenuation coefficient and frequency dependence term of the attenuation coefficient, did not show a clear distinction between the presence of different types of intima layer disease: thickened intima, fibrotic intima, plaque and foam cell. Nevertheless, a more realistic differentiation was obtained with the IBC plots, as presented in Figures 3a-5a. It is possible to differentiate the backscattering characteristics between the layers that constitute the vessel wall. A strong backscattering from both the internal and external elastic lamina was noticed in almost all of the sub-samples. With disease progression, the reflections from the internal and external elastic lamina became less pronounced and the differentiation between media and adventitia and intima became more difficult, as shown in Figure 5a. The IBC varied not only in the same layer, but also among the sub-samples from the same individual sample and, of course, among the samples from different individuals. Table 2 summarizes the IBC values (mean and standard deviation) for all layers.

Despite the small amount of experimental data, the numbers in Table 2 indicate a differentiation between the backscatter co-

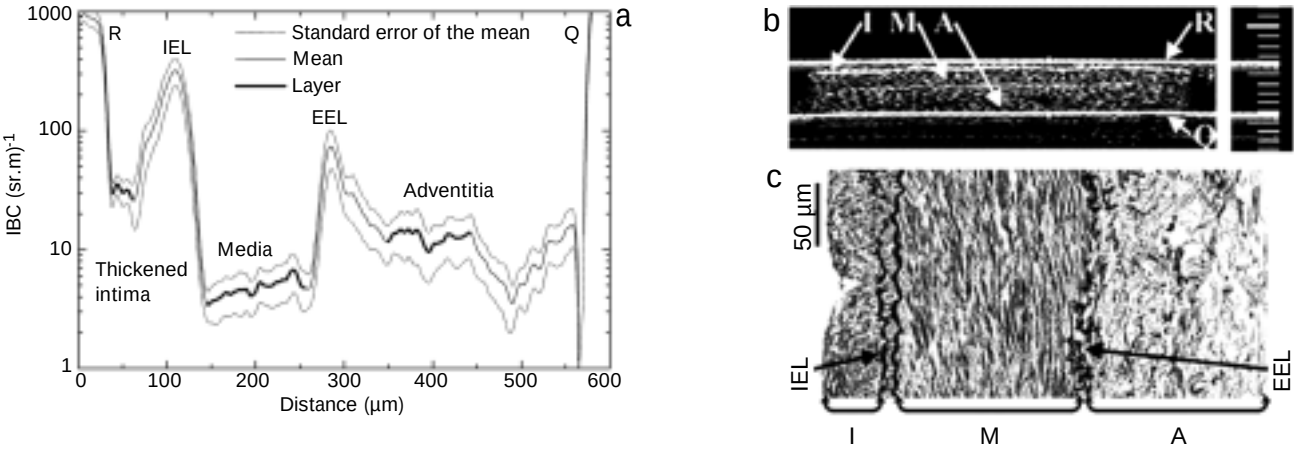

Figure 3. *a*, Integrated backscatter coefficient (IBC) profile across the vessel wall layers; *b*, ultrasound biomicroscope (UBM) image; *c*, histological image of an artery wall including the intima (I) at an early stage of thickening, media (M), adventitia (A), internal (IEL) and external (EEL) elastic lamina. The IBC plot is confined laterally by the reflections from the resinite membrane (R) and quartz plate (Q) shown in *a*. Scale for UBM: 1 div. = 100 µm.

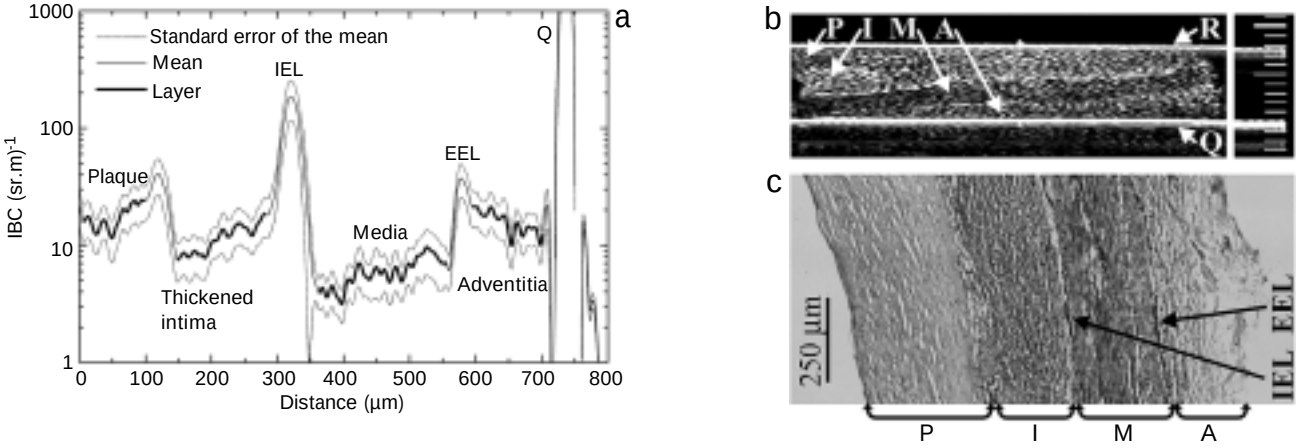

Figure 4. Same as in Figure 3, but for a diseased coronary artery with intimal thickening and deposited plaque (P). Reflection from the resinite membrane is not present in *a*. Scale for UBM: 1 div. = 100 µm.

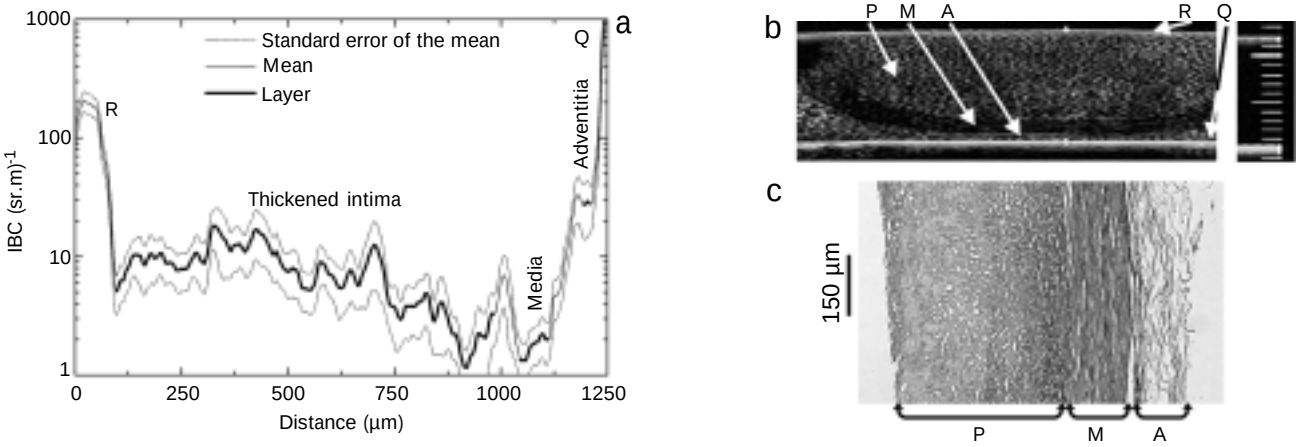

Figure 5. Same as in Figure 3, but for a severely diseased coronary artery. The intima layer is absent and plaque (P) is present. The IBC plot is confined laterally by the reflections from the resinite membrane (R) and quartz plate (Q) shown in *a*. Scale for UBM: 1 div. = 100 µm.

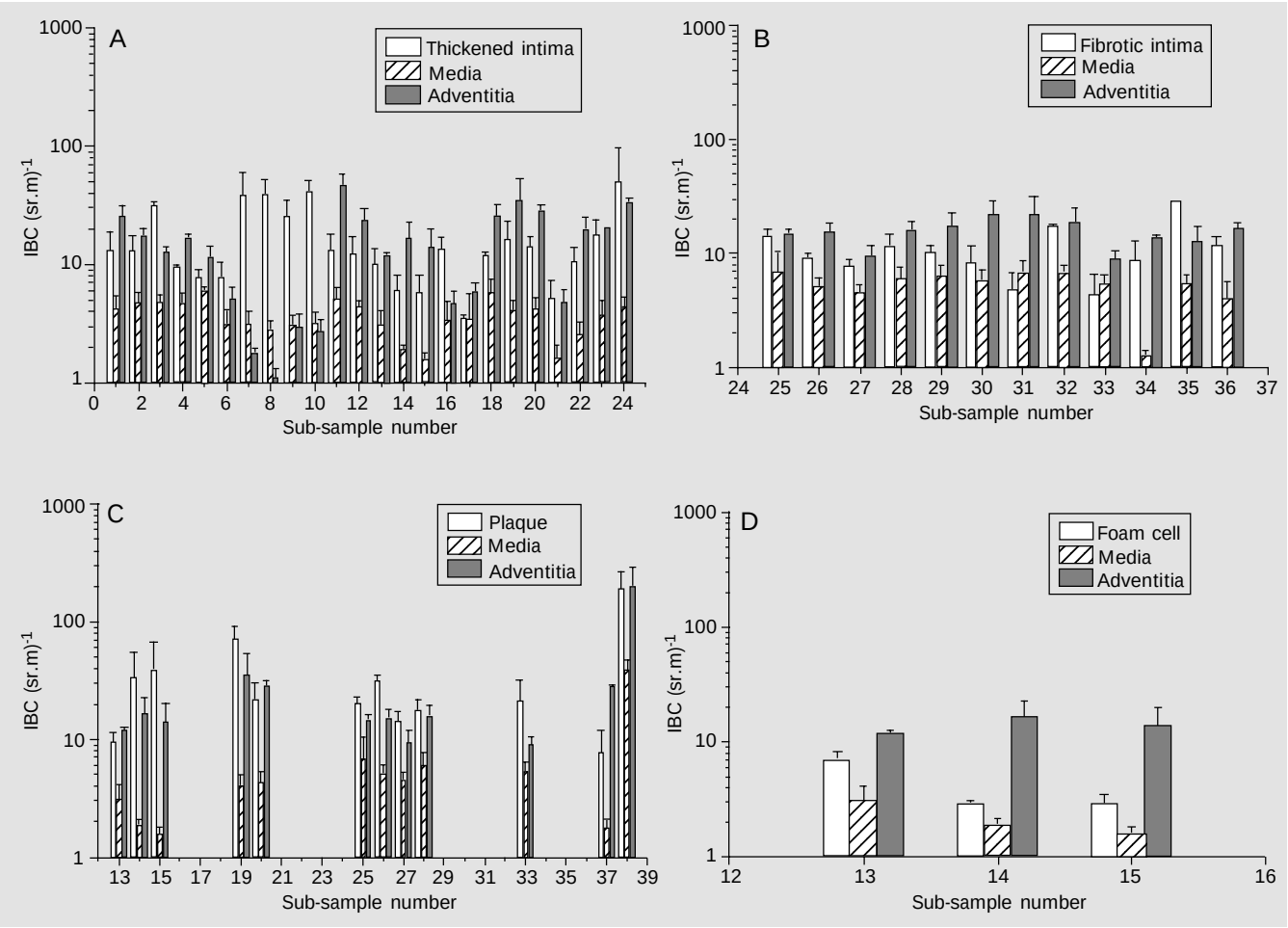

Figure 6. *A*, Bar graph for the integrated backscatter coefficient (IBC) (mean ± SD) of thickened intima, media and adventitia layers of sub-samples 1-24. *B*, Bar graph for the IBC (mean ± SD) of fibrotic intima, media and adventitia layers of sub-samples 25-36. *C*, Bar graph for the IBC (mean ± SD) of plaque, media and adventitia layers of sub-samples 13-15, 19-20, 25-28, 33, and 37-38. *D*, Bar graph for the IBC (mean ± SD) of foam cell, media and adventitia layers of sub-samples 13-15.

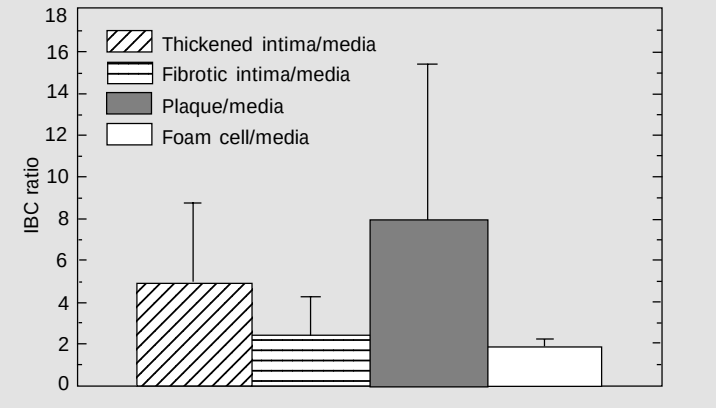

Figure 7. Bar graph for the integrated backscatter coefficient (IBC) ratio (mean ± SD) between thickened intima, fibrotic intima, plaque and foam cell layers and the media layer of corresponding sub-samples.

Table 2. Integrated backscatter coefficient (IBC) for the different layers of the coronary artery sub-samples.

Layer	IBC $(sr.m)^{-1}$	N
Thickened intima	17.42 ± 13.02	24
Fibrotic intima	11.35 ± 6.54	12
Plaque	39.93 ± 50.95	12
Foam cell	4.26 ± 2.34	3
Media	5.12 ± 5.85	38
Adventitia	21.26 ± 31.77	38

Data are reported as means ± SD. N represents the amount of sub-samples in each layer.

efficients of the wall layers. The plaque layer backscatters more signal than all other layers. On the other hand, the media and foam cell layers backscatter less than the other ones. In fact, out of 38 sub-samples only 4 (numbers 7, 8, 9 and 10 in Figure 6A) provided an IBC larger than that for the adventitia layer and only 2 (numbers 31 and 33 in Figure 6B) provided higher IBC than that of the fibrotic intima layer. The IBC for the media layer of human coronary arteries were slightly lower with previous measurements of 20 $(sr.m)^{-1}$ obtained *in vitro* and at 50 MHz by Lockwood et al. (11) for the media layer of human femoral arteries.

The data presented in Table 2 agree with the results shown in Figure 7, which indicate that the normalization of the IBC from one layer with the IBC of the media layer of the same sub-sample tends to compensate for the differences in the backscattering characteristics among sub-samples.

The *t*-test ($P<0.05$) applied to the data of Figure 7 resulted in significantly different means for the IBC ratio of thickened intima/media and fibrotic intima/media. The same result applies to the means of the IBC ratio of fibrotic intima/media and of plaque/media. On the other hand, there was no significant difference between the means of the IBC ratio for the thickened intima/media and for the plaque/media. The test was not applied to the IBC ratio of foam cell/media because of the small number, only three, of experimental results.

In conclusion, this work presented the measurements for the IBC profile of human coronary arteries and the results indicate the possibility to characterize the wall tissue layer by ultrasound.

Acknowledgments

The authors are grateful to Kasia A. Harasiewicz and Peter Faure for technical support, and to the Toronto Hospital for the tissue samples supplied.

References

1. Cotran RS, Kumar V & Robbins SL (1989). Blood vessels. In: Robbins SL (Editor), *Robbins Pathologic Basis of Disease*. 4th edn. W.B. Saunders, Philadelphia, PA, USA.
2. Stary HC (1989). Evolution and progression of atherosclerotic lesions in coronary arteries of children and young adults. *Arteriosclerosis*, 9 (Suppl I): I-19-I-32.
3. Eusterman JH, Achor RWP, Kincaid OW & Brown Jr AL (1962). Atherosclerotic disease of the coronary arteries: A pathologic-radiologic study. *Circulation*, 26: 1288-1295.
4. Mintz GS, Popma JJ, Pichard AD, Kent KM, Salter LF, Chuang YC, Griffin J & Leon MB (1996). Intravascular ultrasound predictors of restenosis after percutaneous transcatheter coronary revascularization. *Journal of the American College of Cardiology*, 27: 1678-1687.
5. Mintz GS, Popma JJ, Pichard AD, Kent KM, Salter LF, Chuang YC, DeFalco RA & Leon MB (1996). Limitations of angiography in the assessment of plaque distribution in coronary artery disease: a systematic study of target lesion eccentricity in 1446 lesions. *Circulation*, 93: 924-931.
6. Landini L, Sarnelli R, Picano E & Salvador M (1986). Evaluation of frequency dependence of backscatter coefficient in normal and atherosclerotic aortic walls. *Ultrasound in Medicine and Biology*, 12: 397-401.
7. Barzilai B, Saffitz JE, Miller JG & Sobel BE (1987). Quantitative ultrasonic characterization of the nature of atherosclerotic plaques in human aorta. *Circulation Research*, 60: 459-463.
8. Greenleaf JF, Duck FA, Samayoa WF & Johnson SA (1974). Ultrasound data acquisition and processing system for atherosclerotic tissue characterization. *Ultrasonics Symposium Proceedings*, 1: 738-743.
9. De Kroon MG, Van Der Wal LF, Gussenhoven WJ & Bom N (1991). Angle-dependent backscatter from the arterial wall. *Ultrasound in Medicine and Biology*, 17: 121-126.
10. Potkin BN, Keren G, Bartorelli AL, Mintz GS & Leon MB (1992). Morphologic characterization of human coronary atherosclerosis by high-frequency intravascular ultrasound. In: Tobis JM & Yock PG (Editors), *Intravascular Ultrasound Imaging*. Churchill Livingstone, New York, NY, USA.
11. Lockwood GR, Ryan LK, Hunt JW & Foster FS (1991). Measurement of the ultrasonic properties of vascular tissues and blood from 35-65 MHz. *Ultrasound in Medicine and Biology*, 17: 653-666.
12. Shepard RK, Miller JG & Wickline SA (1992). Quantification of atherosclerotic plaque composition in cholesterol-fed rabbits with 50-MHz acoustic microscopy. *Arteriosclerosis and Thrombosis*, 12: 1227-1234.
13. Bridal SL, Fornès P, Bruneval P & Berger G (1997). Parametric (integrated backscatter and attenuation) images constructed

using backscattered radio frequency signals (25-56 MHz) from human aortae *in vitro*. *Ultrasound in Medicine and Biology*, 23: 215-229.

14. Foster FS, Knapik DA, Machado JC, Ryan LK & Nissen SE (1997). High frequency intracoronary ultrasound imaging. *Seminars in Interventional Cardiology*, 2: 33-41.
15. Bridal SK, Tousaint JF, Raynaud JS, Fornès P, Willig AL & Berger G (1998). US backscatter and attenuation 30 to 50 MHz and MR T2 at 3 tesla for differentiation of atherosclerotic artery constituents *in vitro*. *IEEE Transactions on Ultrasonics Ferroelectrics and Frequency Control*, 45: 1517-1525.
16. Machado JC & Foster FS (2001). Ultrasonic integrated backscatter coefficient profiling of human coronary arteries *in vitro*. *IEEE Transactions on Ultrasonics Ferroelectrics and Frequency Control*, 48: 17-27.
17. D'Astous FT & Foster FS (1986). Frequency dependence of ultrasound attenuation and backscatter in breast tissue. *Ultrasound in Medicine and Biology*, 12: 795-808.
18. Foster FS, Strban M & Austin G (1984). The ultrasound microscope: initial studies of breast tissue. *Ultrasound Imaging*, 6: 243-261.
19. Foster FS, Pavlin CJ, Harasiewicz KA, Christopher DA & Turnbull DH (2000). Advances in ultrasound biomicroscopy. *Ultrasound in Medicine and Biology*, 26: 1-27.
20. Ye SG, Harasiewicz KA, Pavlin CJ & Foster FS (1995). Ultrasound characterization of normal ocular tissue in the frequency range from 50 MHz to 100 MHz. *IEEE Transactions on Ultrasonics Ferroelectrics and Frequency Control*, 42: 8-14.